The unusual infrared colors of a faint object in the Chamaeleon I star forming region[1]

F. Comerón

European Southern Observatory, Karl-Schwarzschild-Strasse 2, D-85748 Garching bei München, Germany

fcomeron@eso.org

and

P. Claes

European Space Agency, ESTEC/APP-NSG, NL-2200 AG Noordwijk, The Netherlands

pclaes@estec.esa.int

Received ______________________; accepted ______________________

ABSTRACT

We present deep near-infrared ($J_S H K_S$) imaging observations carried out with the ESO Very Large Telescope (VLT) of a field in the Chamaeleon I star forming region in an attempt to identify possible members with masses comparable to, or below, the mass of Jupiter. We focus on an object, ChaI J110814.2-773649, which stands out as an outlier in color-color and color-magnitude diagrams of the field, with $H = 22.16^{+0.21}_{-0.17}$, $H - K_S = -0.01^{+0.26}_{-0.24}$, $J_S - H = 2.00^{+\infty}_{-0.62}$. H-band spectroscopy of this object shows that the unusual colors are not due to emission lines in that region, and even provide a clear detection of its continuum. Assuming membership in Chamaeleon I and an age of 2 Myr like for the bulk of the members of that region, the blue $H - K_S$ color and the absolute magnitude are consistent with model predictions for a cool, sub-Jupiter mass object with strong dust depletion in the atmosphere. However, the very red $J_S - H$ color implied by the marginal detection in the J_S band is unexpected in an object with such atmospheric properties. We speculate that this might be due to differences in the properties of dust and its depletion under the photosphere with respect to field objects (T dwarfs) with a similar temperature, resulting from both the youth and the low surface gravity of a low mass member of a star forming region. We also consider the alternative possibility that ChaI J110814.2-773649 might actually be a high redshift object, whose red $J_S - H$ color could result from absorption of the flux bluewards of Lyman α in the J band. We find that such possibility would be marginally compatible with the $J_S H K_S$ photometry of ChaI J110814.2-773649 if it were an unreddened starburst at $8.5 < z < 11$.

Subject headings: stars: low-mass, brown dwarfs — stars: formation

1. Introduction

The search for the bottom of the stellar mass function, one of the main goals of surveys of star forming regions just less than one decade ago (Tinney 1995), has been replaced now by the search for objects beyond the bottom of the brown dwarf mass function and the ultimate limit below which compact objects cannot form in isolation. The realization that freely-floating objects keep being found as surveys probe lower and lower masses (Zapatero Osorio et al. 1999, 2000, 2002; Martín & Zapatero-Osorio 2003; Lucas & Roche 2000; Lucas et al. 2001) has forced to rethink object formation theories (Reipurth and Clarke 2001; Boss 2001) and even the basic definitions and nomenclature that apply to objects not orbiting a larger body and whose mass is near or below the deuterium-burning limit of $\simeq 12\ M_J$ (Saumon et al. 1996). Despite recent progress, the direct detection of truly Jupiter-mass and even lighter objects outside our Solar System remains an observational challenge pushing current instrumental capabilities to their limits.

The complex molecular and dust chemistry in the atmospheres of objects with temperatures near $T \sim 1000$ K causes major flux redistributions that increase by orders of magnitude the near-infrared brightness with respect to black bodies, and produce highly peculiar colors that are difficult to mimic by any other astrophysical objects (Burrows et al. 1997). These two properties suggest that such cool objects may be relatively easy to detect thanks to their brightness, and to recognize thanks to their colors. Actual observations of objects with spectral type T (Kirkpatrick et al. 1999), brown dwarfs much cooler than the coolest stars, confirm the main results of theoretical modelling (Burgasser et al. 1999; Leggett et al. 2000; Chabrier et al. 2000; Burrows et al. 2001; Dahn et al. 2002). The large age difference between million-years-old star forming regions and the gigayears-old

---

[1]Based on observations obtained at the European Southern Observatory using the the Very Large Telescope, Cerro Paranal, Chile (programmes 64.L-0049(A) and 67.C-0109(B))

field population implies dramatic differences between the masses of newly formed and of evolved T-dwarf-like objects: while a brown dwarf of 40 Jupiter masses (M_J) reaches the temperature of $\simeq 1200$ K marking the approximate boundary between L and T dwarfs (Burgasser et al. 2002a) at the age of 1 Gyr, the same temperature corresponds to a mass around 5 M_J at the age of 10 Myr, and to less than 2 M_J at 1 Myr (Baraffe et al. 2003). The near-infrared luminosities predicted by models indicate that T-dwarf-like objects in the nearest star forming regions should be within the reach of current instrumentation in 4- to 8-meter class telescopes, as confirmed by the recent discovery of a possible member of the σ Ori aggregate with T-dwarf-like spectral features (Zapatero Osorio et al. 2002). However, the faint magnitudes that such observations need to reach also extend the horizon to high-z objects with appearances very different from those of objects in the local Universe, thus requiring extra care in the interpretation of objects with unusual colors.

This paper presents observations carried out with the ESO Very Large Telescope (VLT) of a very faint object in the direction of the Chamaeleon I star forming region with highly unusual infrared colors, characterized by a blue $H - K_S$ index combined with a very red $J_S - H$. Spectroscopy demonstrates that these colors are due to a continuum spectrum, and not to the presence of emission lines in the H band. We hypothesize that the object might be a very low mass member of Chamaeleon I, whose faintness would then suggest an extremely low, possibly sub-Jupiter mass that would make it the least massive compact object detected so far outside the Solar System. However, we also contemplate the possibility that the object might be an extremely high-z object, finding marginal consistency between its colors and those expected from an unobscured starburst at a redshift $z > 8.5$ that would make it a J-band dropout.

2. Observations and data reduction

The Chamaeleon I cloud, at 160 pc from the Sun (Wichmann et al. 1998), is one of the nearest star forming regions. Besides its proximity, other factors make it an attractive target for the study of its lowest mass contents: the low internal extinction over most of its subtended area yields a mostly unobscured view of its contents, and its moderately high galactic latitude (18° South of the galactic plane) decreases the density of background sources. Moreover, several very low mass stellar and substellar members have been already detected there with masses down to $20 - 30$ M_J (Comerón et al. 2000, 2003), thus encouraging the search for even lower mass objects.

2.1. Imaging

We obtained deep imaging in the J_S, H, and K_S bands of a field covering 2.5×2.5 $arcmin^2$ on the sky using ISAAC, the infrared imager and spectrograph at the VLT, on the nights of 2000 March 27 and 28. The field is centered at $\alpha(2000) = 11^h08^m16^s\!.5$, $\delta(2000) = -77°35'36''$, and was chosen because of the existence of previously identified brown dwarf candidates in its proximity (Comerón et al. 2000), while avoiding regions of high extinction and bright nearby stars that might produce ghost images on the detector.

The images were obtained by integrating on the field for approximately 30 minutes in a given filter, splitting the integration into several individual exposures obtained with telescope offsets of a few tens of arcseconds in between. We then switched to a different filter and repeated the procedure. The observations in each of the three filters were distributed along our two observing nights to average over time any possible source variability with timescales shorter than the span of our observing run. Each block of integrations in each filter was combined into a single image, in which the individual frames were reduced by subtracting a sky frame (constructed by median averaging of the field frames uncorrected for telescope offsets, so as to remove the source images and cosmic ray hits) and dividing by a master flat field based on sequences of twilight sky exposures with different illumination levels. All the blocks in each filter were then combined into a deep image of the field, by means of an average in which the contribution of each individual block was weighted with the inverse square of the dispersion of the counts of its background. In this way, "noisy" frames obtained with relatively high background levels had a reduced contribution to the average. Total exposure times were 2.7 hours in J_S, 2.5 in H, and 7.9 in K_S. The longer exposure times in K_S are due to the blue $H - K_S$ indices expected for the objects of interest in this work.

The targeted region does not show any obvious nebulosity in the visible and, given the progressively lower efficiency of scattering by small dust grains towards longer wavelengths, the visibility of any possible remaining faint nebulosity at infrared wavelengths is expected to be even lower. Indeed, tenuous filamentary nebulosity across the field is perceptible only in the final combined images, most clearly in the J_S image. The sky frame constructed according to the procedure described above effectively filters out extended, uniform nebulosity as well as point sources and small extended sources. However, it would leave unfiltered any nebulosity with brightness variations over angular scales comparable to the amplitude of the offset pattern, which would then be apparent in the sky-subtracted frames as zones with local negative backgrounds, and may bias in this way the flux estimates of the detected sources. No such effect is at all seen in our images, thus giving us confidence that the sky subtraction procedure followed is well suited for the reduction of our target field.

Photometric calibration was performed by observing at the beginning of each night the standard star S064-F, lying near the Chamaeleon I region, followed by an observation of the target field at a nearly identical airmass. This standard is a part of the set that defines the Las Campanas/Palomar NICMOS system (Persson et al. 1998), which the broad-band filter plus detector system of ISAAC match well. This allowed us to establish a network of local secondary standards, which were used to determine the photometric zeropoints of the deep images. We then stacked together the three deep frames in each filter, and used the DAOFIND task under the DAOPHOT package (Stetson 1987), available in IRAF[2], for automated source detection. Photometry was performed by point-spread function (PSF) fitting using as a reference for the PSF determination the brightest point sources in the field, using the DAOPHOT PEAK task. After experimenting with different PSF functional forms available under the DAOPARS package a PSF consisting of a Gaussian analytical part plus a lookup table of residuals, both constant across the field, was chosen. Comparison with the results obtained using other forms for the analytical component showed no major differences in the results. The measured FWHM of the PSF in the combined images is $0''81$ (J_S), $0''71$ (H), and $0''66$ (K_S). Since the photometry was performed by fitting of a stellar PSF it is accurate only for point sources, which are the objects of interest in this work. Photometric errors and detection limits for point sources were derived by adding artificial stars to the frames, constructed by scaling the derived PSF according to the desired magnitude, and then recovering their photometry in the same way as for the real stars. The errors quoted thus correspond to the 1-σ scatter in the input magnitudes of the artificial stars that produce a given recovered magnitude. We obtain average 5σ detection limits for point sources of $J_S = 23.20$, $H = 22.30$, $K_S = 22.35$, with slight regional variations below the 0.1 mag level due to the presence of faint filamentary nebulosity across the field.

Figure 1 shows the $(H - K_S, H)$ color-magnitude diagram of all the sources detected in our images having a detection above the 3σ level in at least one of the bands. At the bright

---

[2]IRAF is distributed by NOAO, which is operated by the Association of Universities for Research in Astronomy, Inc., under contract to the National Science Foundation

end ($H < 18$) late-type stars, with a narrow range of colors and a well defined blue boundary at $H - K_S \simeq 0.3$, dominate. Both the narrowness of the range and the low value of the $(H - K_S)$ index show that the extinction is low and fairly uniform throughout the region. This is confirmed by the color-color magnitude (Figure 2), where most objects cluster at the colors expected for mid-to-late type stellar photospheres reddened by extinctions between 0.2 and 0.6 mag at K_S.

At fainter magnitudes extragalactic sources, generally redder and often resolved, progressively take over. However, there is an obvious outlier at $H - K_S = -0.01^{+0.26}_{-0.24}$, $H = 22.16^{+0.21}_{-0.17}$. The object (hereafter referred to as ChaI J110814.2-773649 after its J2000 equatorial coordinates) is at most barely detected at $J_S \simeq 24.16^{+\infty}_{-0.59}$, implying $J_S - H = 2.00^{+\infty}_{-0.62}$.

Even though measurement uncertainties are marginally compatible with a $(H - K_S)$ color close to the blue boundary defined by the other sources in the field, its combination with the high upper limit in $(J_S - H)$ implies very unusual near-infrared colors for ChaI J110814.2-773649. This is more clearly visible in Figure 2, where the separation of ChaI J110814.2-773649 with respect to all the other objects in the field is very clear. No other objects with comparable photometric properties are detected in the field. Figure 3 shows a small section of the field centered on ChaI J110814.2-773649 in the three bands. The fact that it is clearly seen at H but hardly at J_S would anticipate a considerable brightness at K_S but, as can be seen by comparing to the objects surrounding it, this does not happen. A comparison with the radial plots of the PSF reference stars does not show any evidence for ChaI J110814.2-773649 being spatially extended.

2.2. Spectroscopy

The photometric properties of ChaI J110814.2-773649 are highly unusual for an object with a continuum-dominated spectrum, but they might be reproduced by a AGN or QSO with intense emission lines conveniently redshifted (vanden Berk et al. 2001): one or a few strong lines in the H band would make the object appear red in $J_S - H$ and blue in $H - K_S$. Obvious candidates are Hα redshifted to $z \simeq 1.5$, Hβ+[OIII] to $z \simeq 2.3$, or [OII] to $z \simeq 3.4$.

We obtained a 10-hours-long H band spectrum of ChaI J110814.2-773649, also using ISAAC at the VLT, on the nights of 2001 April 29 and May 1. The goal was to discern between the possibilities of emission lines dominating the H-band flux of the object (which should be relatively straightforward to detect in such a deep spectrum) and of an unusual continuum spectral energy distribution (which should result in a non-detection of the object, or a marginal detection at most, due to the spread of the flux over the spectral range covered). We were fortunate to enjoy excellent transparency conditions and subarcsecond seeing during virtually the entire time devoted to these observations.

Individual spectra were obtained with the $1''0$ slit oriented so as to include in it a brighter, $H = 16.83$ reference star located $16''$ from ChaI J110814.2-773649. A total of 200 individual spectra of 180 seconds of exposure time each were obtained with nodding along the slit combined with a small random offset around each of the two nod positions. The presence of the reference star provides an easy way to monitor the object centering during the integrations and to correct for telescope nodding at the reduction stage, and it also includes in each frame a secondary calibrator for telluric absorption correction. Consecutive frames taken at two different nod positions were subtracted to cancel sky emission lines, and then divided by a spectroscopic flat field frame constructed from calibration frames taken with an internal continuum lamp respectively switched on and off. We refer in what follows to these sky-subtracted, flat-fielded frames as "pairwise-subtracted frames".

At the time when our observations were obtained, ISAAC suffered from a pickup noise problem that imposed a wave pattern along detector columns, corresponding to the spatial direction. The amplitude of the pattern is far too low to be seen in the individual pairwise-subtracted frames, where it is hidden by the background and readout noise. However, it becomes readily apparent at the very high sensitivity levels obtained when coadding the 200 pairwise-subtracted frames after correcting for the telescope nodding using as reference the trace of the spectrum of the bright star. We removed this pattern by adopting an additional step in the data reduction, which consisted of subtracting from each pairwise-subtracted frame another frame containing almost uniquely the wave pattern. To do this, we took advantage of the fact that the wavelength of the pickup noise pattern was almost exactly 6.5 pixels along the spatial direction. We thus produced a wave pattern frame by combining and median-filtering the pairwise-subtracted frame with copies of itself shifted respectively by 13, 26, 39, 52, 65, and 78 pixels along the detector columns, and trimming it to the same dimensions of the original image. Then, we subtracted this wave pattern frame from the pairwise-subtracted frame from which it was produced. In this way, the deep spectroscopic frame obtained by combining the pairwise-subtracted, wave pattern-subtracted frames after correcting for the telescope nodding contains no detectable trace of the pickup noise, thus greatly increasing the visibility of possible spectral traces of extremely faint objects.

3. Discussion

3.1. The spectrum of ChaI J110814.2-773649

Examination of the deep spectroscopic frame that combines our 10 hours of integration shows no hints of emission lines at the expected position of the spectrum of ChaI J110814.2-773649, while it is possible to show that the sensitivity of this frame should be sufficient to easily reveal any emission lines dominating the H-band flux. The background noise in the spectroscopic frame greatly varies depending on whether or not strong OH airglow lines are present at the corresponding wavelength. On the other hand, the spectrum of the $H = 16.83$ reference star allows us to perform an approximate flux calibration and thus determine the number of counts that should be expected in a single line dominating the emission. In this way, we find that if the H-band flux of ChaI J110814.2-773649 were contributed by a single line with a Gaussian profile peaking at the wavelength most affected by airglow emission, its full-width at half maximum should exceed 360 Å so that its peak intensity integrated over the spatial profile would fall below 3 times the local background noise at that detector column. Such width would correspond to a rest frame line width of 145 Å for Hα at $z = 1.5$, 110 Å for Hβ or [OIII] at $z = 2.3$, or 82 Å for [OII] at $z = 3.4$. For Hα or Hβ these values are about three times greater than those found in typical QSO spectra (vanden Berk et al. 2001). The discrepancy would be smaller for Lyα, whose corresponding rest frame width would be only 27 Å, although the redshift of that line into the H band would then imply $10.6 < z < 13.8$. We should keep in mind nevertheless that these are are deliberately conservative limits that are made even more stringent (i.e., involving greater intrinsic widths) if we assume that the line peaks in a region less affected by skyglow. Similarly, such large widths greatly exceed those of the telluric OH line blends, thus implying intensities comparable to the peak one also at wavelengths where airglow lines are absent and the background noise is thus much lower. We thus consider that our spectrum effectively excludes the possibility that the H band flux of ChaI J110814.2-773649 may be dominated by line emission.

In view of the non-detection of sufficiently strong emission lines to account for the H band detection, we decided to boost up the sensitivity to attempt the detection of the continuum by strongly binning the spectrum along the dispersion direction. The 1024 detector columns were thus collapsed into 20 bins. Each column contributed to the bin with a weight inversely proportional to the squared dispersion of the counts along it (excluding the regions affected by the trace of the reference star or by the artifacts that it produced when building the wave pattern frame), so as to reduce the contribution of those wavelengths affected by the presence of sky airglow lines. The binned spectrum is shown in Figure 4, where we have indicated the position where the trace of the spectrum of ChaI 110814.2-773649 should be expected. Indeed, a slight increase of the number of counts over the background can be appreciated at precisely that position, especially on the left half of the frame corresponding to shorter wavelengths. The excess of counts is detectable over several bins and its peak along the spatial direction seems to be parallel to the trace of the spectrum of the reference star. We thus consider it as the actual detection of the spectrum of ChaI 110814.2-773649, demonstrating that the H band is indeed dominated by continuum emission and that the unusual colors of this object are due to an exotic spectral energy distribution rather than to the presence of emission lines.

3.2. The nature of ChaI J110814.2-773649

3.2.1. An extremely high-z galaxy?

The existence of an object with the colors of ChaI J110814.2-773649 in exposures like the ones presented here must be interpreted with caution. On the one hand, such deep images have the potential of detecting objects spanning a wide range of redshifts, sampling the rest-frame ultraviolet spectrum of objects in early evolutionary stages that are absent from the local Universe, and thus being sensitive to sources with colors widely different from those characteristic of brighter, and typically more nearby, objects. On the other hand, observations of fields in the JHK_S bands to a depth comparable to that of our observations are still scarce, although recent and ongoing efforts such as the deep JHK_S imaging of the Hubble Deep Field South (HDFS) (Labbé et al. 2003), the MS1054-03 cluster (Franx et al.

2000) or the multiband imaging of the Chandra Deep Field South (Renzini et al. 2003) are providing valuable information on the near-infrared colors found at such faint magnitudes. Other deep near-infrared surveys recently carried out with 8m-class telescopes, such as the Subaru Deep Field (Maihara et al. 2001) have tended to use the J and K_S bands alone, due to their focus on the detection of very red objects. As a result, the framework for comparison of our results, especially concerning objects with unusual colors such as ChaI J110814.2-773649, is still rather limited. In any case, a comparison to published JHK_S data for the HDFS over a similar field of view (Labbé et al. 2003) does confirm that the colors of ChaI J110814.2-773649 are quite unique, despite of the fact that the HDFS survey reaches down to limiting magnitudes (3σ) that are respectively 1.6 (J_S), 2.7 (H), and 2.2 (K_S) fainter than those of ChaI J110814.2-773649.

No objects with similar colors are detected either in deep infrared images of the Hubble Deep Field North (HDFN), although the presence of an object with very atypical colors, HDFN-JD1, has been reported by Dickinson et al. (2000) in near-infrared images of that field. The object in the HDFN is outstanding because of its very red $H - K$ color and for being undetected at J, thus being by far the reddest object in the field in $J - H$. Although HDFN-JD1 may be considered as the opposite of ChaI J110814.2-773649 as far as $H - K$ is concerned (HDFN-JD1 being extremely red, while ChaI J110814.2-773649 is unusually blue), the large $J - H$ values are puzzling in both cases. It is interesting in this respect to consider Figure 7 of that paper, which considers the variation of the $J - H$ and $H - K_S$ colors with redshift for a number of galaxy types modelled after the spectral energy distributions of Bruzual and Charlot (1993). The curves presented there range from a passively evolving elliptical galaxy formed at $z = 15$ to a unreddened starburst galaxy, and can be considered as bracketting the entire range of colors encountered among extragalactic objects. The bluest ($H - K_S$) colors predicted by such models are produced by unreddened starbursts, reaching $(H - K_S) \simeq +0.2$ [3] near $z = 2.5$ and $z = 5.5$. Such redshifts are however ruled out by the very blue $(J_S - H)$ predicted in both cases, which are incompatible with the extremely red $(J_S - H)$ of ChaI J110814.2-773649. At larger redshifts the Lyα forest enters the near infrared, progressively decreasing the flux in the J band. At $z = 8.5$ and greater the flux depletion on the blue side of the J band moves the $(J_S - H)$ color above 1.4, thus becoming compatible with our lower limit, while still maintaining a relatively blue $(H - K_S)$ at 0.35 mag. Similarly blue $(H - K_S)$ colors and ever redder $(J_S - H)$ colors are predicted as the starburst is shifted up to $z \simeq 11$, where Lyα enters the H band and starts reddening $(H - K_S)$ as well. While the error bars of our observations do not completely exclude $(H - K_S) = 0.35$ for ChaI J110814.2-773649 it must be recalled that, as noted in Section 2.1, a foreground extinction of at least 0.2 mag caused by dust in the Chamaeleon I cloud pervades the field, thus reddening any background objects by at least 0.1 mag in $(H - K_S)$. The bluest high-redshift starbursts should thus have $(H - K_S) > 0.45$, which we consider hardly compatible with our measured fluxes. In summary, we consider an unreddened starburst at $8.5 < z < 11$ as a marginally consistent explanation for the unusual colors of ChaI J110814.2-773649, based on arguments similar to the ones that lead Dickinson et al. (2000) to propose a $z = 12.5$ object as a possible interpretation of HDFN-JD1.

3.2.2. A young planetary-mass object?

Although an extremely high redshift object may indeed account for the spectral energy distribution of ChaI J110814.2-773649, the serendipity of our finding and its location in the

[3] The AB magnitudes used by Dickinson et al. (2000) have been transformed into the Vega magnitudes used throughout this paper for comparison.

direction of a nearby star forming region leads us to consider also the possibility that it may be a young, isolated planetary mass member of Chamaeleon I. Near-infrared spectra of T-dwarf-like objects are dominated by strong molecular absorption caused by CH_4, H_2O, and H_2, producing a broad-band spectral energy distribution characterized by blue $J-H$, $H-K$ colors. At the somewhat higher temperatures of L-type dwarfs dust is present in the atmosphere in the form of clouds containing a complex mixture of metals and minerals (Burrows et al. 2001), producing instead extremely red colors. The disruption of clouds and precipitation of its condensates below the photosphere is thought to happen over a relatively narrow margin of temperatures around $T \simeq 1200\ K$ (Burgasser et al. 2002a), marking the transition between the L and T spectral types.

The tracks overplotted in Figure 1 represent the colors and magnitudes expected for young L- and T-dwarf-like objects at the distance of Chamaeleon I, after the evolutionary tracks of Chabrier et al. (2000) (DUSTY models) and Baraffe et al. (2003) (COND models). The former (dashed lines in the figure) are expected to represent L-dwarf-like, dusty atmospheres, appropriate for objects hotter than $T \simeq 1200\ K$, while the latter reproduce the characteristics of cooler objects in which dust has precipitated below the photosphere. The transition temperature between the DUSTY and the COND tracks is attained at a H magnitude between 18.5 and 19.2 on the COND tracks, and between 20.5 and 21.3 on the DUSTY tracks. The magnitude intervals quoted reflect the mild age dependence of the temperature-magnitude relationship over the $1-10\ Myr$ range. As seen in Figure 1, both the faint H magnitude of ChaI J110814.2-773649 and its location offset bluewards from the general distribution of objects in the color-magnitude diagram can be well reproduced by an extremely low mass member of the star forming region. This is fairly independent of the assumed age, due to the broad overlap of the tracks. However, the assigned mass does depend strongly on the age, as the symbols indicating the location of objects with a given mass show. Remarkably, adopting the age that best reproduces the locations of very low mass stars and massive brown dwarfs in Chamaeleon I, 2 Myr, yields a mass of only $\sim 0.7\ M_J$ for ChaI J110814.2-773649, or about two Saturn masses. The spectrum of the object (Figure 5) displays hints of a possible peak around 1.55 Å followed by a drop to near zero emission levels at longer wavelengths, consistent with the overall spectral energy distribution of T dwarfs that also peaks at the same position. However, the extremely low signal in the spectrum makes the actual existence of the peak doubtful. It should be pointed out too that the rise near 1.8 μm, if real, would have no correspondence in T dwarf spectra, thus casting doubts on this interpretation.

The agreement of the H and K_S photometry with models of very young T-dwarf-like objects does not hold when we consider the $J_S - H$ color as well, which is generally close to zero in T dwarf spectra. As seen in the color-color diagram of Figure 2, while $H - K_S$ is fully within the range expected for a T-dwarf-like object, the $J_S - K_S > 1.4$ of ChaI J110814.2-773649 seems instead characteristic of a cool L dwarf. In this respect, the photometric properties of ChaI J110814.2-773649 qualitatively resemble those of transition objects between the L and T types observed by Leggett et al. (2000), which are attributed to the persistence of dust in the atmosphere coexisting with the onset of strong CH_4 absorption in the K band. The sequence of colors along this transition is not well known, as it depends on factors such as the partial disruption of clouds (Burgasser et al. 2002a), the composition of grains (Lodders 1999), and their size distribution, which in turn are sensitive functions of the surface gravity (Cooper et al. 2003). The low gravity of cool young planetary mass objects, over two orders of magnitude lower than that of the field, evolved objects with which models have been mainly confronted so far, also imply important structural differences in both the atmosphere and the layers beneath the photosphere. The lower gravity brings convection much closer to the photosphere than in evolved T dwarfs (Burrows et al. 1997), thus facilitating the presence of small grains in the atmosphere due to convective overshooting or turbulent diffusion (Chabrier & Baraffe

2000) at temperatures under which they would be absent in more evolved objects. All these factors might account for the maintenance of hybrid features such as L-dwarf-like reddening at $J_S - H$ and T-dwarf-like bluening at $H - K_S$ at even lower temperatures and luminosities in young planetary-mass objects, accounting for the observed colors of ChaI J110814.2-773649 despite a brightness that is well below that predicted for a young early-T object. At this point this is a very speculative explanation unsupported by proper modelling, but the identification of such hybrid features as being common among other young very low mass objects could lend support to it.

It is interesting in this respect to compare ChaI J110814.2-773649 with S Ori 70, a confirmed T dwarf-like object recently discovered by Zapatero Osorio et al. (2002) in the direction of the σ Ori association. The membership, and therefore the youth, is considered as likely by these authors based on both probabilistic arguments derived from the actual density of similar objects in the field, and on fits to theoretical spectra with different surface gravities, which tend to give a better match for low surface gravity values. This has been recently confirmed by Martín & Zapatero-Osorio (2003) based on mid-resolution infrared spectroscopy. This object is considerably brighter than ChaI J110814.2-773649 despite of the distance of σ Ori, over twice as large as that of Chamaeleon I: if both are members of their respective star forming regions, the difference in absolute H magnitudes is about 3.5 mag. Interestingly, S Ori 70 also has unusual colors for a T dwarf-like object, albeit in a different sense as ChaI J110814.2-773649: while the $J - H$ colors of S Ori 70 is very blue and consistent with those of field T dwarfs, its $H - K$ is unusually red when compared to an object of this class (Dahn et al. 2002; Leggett et al. 2002) as well as to the best-fitting theoretical models. Moreover, its brightness places it between 1 and 2 magnitudes above the sequence predicted by models in color-magnitude diagrams for objects of the same color. The spectroscopic confirmation of S Ori 70 as a T dwarf-like object and its likely membership in the σ Ori thus cautions about the diversity found among otherwise similar objects of this kind, and the limited reliance that must be placed on the models.

4. Conclusions

In this paper we have reported the discovery with the ESO Very Large Telescope of an object in the direction of the Chamaeleon I star forming region, ChaI J110814.2-773649, characterized by its unusual near-infrared colors. The object is faint ($H = 22.16^{+0.21}_{-0.17}$), very red in $J_S - H$ ($2.00^{+\infty}_{-0.62}$), and very blue in $H - K_S$ ($-0.01^{+0.26}_{-0.24}$). A 10h long H-band spectrum demonstrates that the colors are not due to the presence of strong emission lines in the H band, and actually reveals the continuum of the object.

We consider two possible interpretations for ChaI J110814.2-773649. In the first one, corresponding to a very high redshift object, a marginally acceptable match to the colors is found by assuming that ChaI J110814.2-773649 is an unreddened starburst turned into a J-band dropout by its extremely high redshift ($8.5 < z < 11$) that makes the Lyα forest penetrate well into the J band. Other spectral energy distributions at different, lower redshifts cannot simultaneously reproduce both the red $J_S - H$ and the blue $H - K_S$ colors. The very high redshift implied by this explanation, which greatly exceeds that of any spectroscopically confirmed source known so far, and the important quantitative difference between the bluest ($H - K_S$) color allowed by the models and the observed one makes us consider it quite unlikely.

The second explanation, motivated by the location of ChaI J110814.2-773649 in the general direction of the Chamaeleon I cloud, is that it may be an actual very low mass member of that region. Taken together, the $H - K_S$ color and the H magnitude are consistent with the model predictions for a planetary mass object of roughly 0.7 Jupiter masses with an age of 2 Myr, or slightly above one Jupiter mass if it is 5 Myr old. However, this explanation does not seem consistent with the very red $J_S - H$ implied by the marginal detection at J_S, which models predict only for the coolest dusty atmospheres. We speculate that ChaI J110814.2-773649 might be an object with spectral features hybrid between those of L and T dwarfs, displaying both a dusty atmosphere that reddens $J_S - H$ while at the same time having strong CH_4 bands that make $H - K_S$ blue, with the coexistence of both features being possible due to the low surface gravity of such a young object.

Both possible explanations are quite exciting: the first one would imply that ChaI J110814.2-773649 is a record-breaking high redshift object, while the second one would make it the least massive compact object so far identified outside the solar system. It is thus tantalizing not being able to distinguish between both radically different possibilities with the data currently at hand, and it must be kept in mind that the subsisting photometric uncertainties do not completely exclude other less exotic possibilities. Further ground-based spectroscopy will demand great amounts of integration time at the largest telescopes, and detection at longer wavelengths must wait for the next generation of spaceborne infrared observatories (Burrows et al. 2001). However, new observations of ChaI 110814.2-773649 and other possible new young, isolated planetary-mass objects with currently available means are important. A better determination of the unusual colors of ChaI 110814.2-773649 and monitoring for variability are obvious follow-up tasks, while astrometry, which could confirm kinematical membership over a timescale of 5-10 years, would address the origin of ChaI 110814.2-773649 as either an isolated object or as a former planet expelled from its parent stellar system (de la Fuente Marcos & de la Fuente Marcos 1998; Reipurth and Clarke 2001). Finally, new deep searches in star forming regions will tell us if young, isolated planetary mass objects are a common outcome of stellar and planetary system formation, or rather a rarity among astrophysical objects.

We are very pleased to thank Dr. Adam Burrows for providing details on his model calculations and for a critical reading of an earlier version of this manuscript. Drs. France Allard and Isabelle Baraffe are thanked for useful remarks on the validity of the Baraffe et al. (2003) model predictions at the very young ages of relevance here. Insightful comments by the referee, Dr. Phil Lucas, as well as a second anonymous referee, and the editor, Dr. James Liebert, helped improving this paper in both contents and presentation. Last but not least, the excellent support received from the Paranal Science Operations staff during our VLT observations in 2000 and 2001 is warmly appreciated.

REFERENCES

vanden Berk, D.E., Richards, G.T., Bauer, A., et al., 2001, AJ, 122, 549.

Baraffe, I., Chabrier, G., Barman, T.S., Allard, F., Hauschildt, P.H., 2003, A&A, 402, 701.

Bessell, M.S., Brett, J.M., PASP, 100, 1134.

Boss, A.P., 2001, ApJ, 551, L167.

Bruzual, G., Charlot, S., 1993, ApJ, 405, 538.

Burgasser, A.J., Kirkpatrick, J.D., Brown, M.E., Reid, I.N., Gizis, J.E., Dahn, C.C., Monet, D.G., Beichman, C.A., Liebert, J., Cutri, R.M., Skrutskie, M.F., 1999, ApJ, 552, L65.

Burgasser, A.J., Marley, M.S., Ackerman, A.S., Saumon, D., Lodders, K., Dahn, C.C., Harris, H.C., Kirkpatrick, J.D., 2002a, ApJ, 571, L151.

Burgasser, A.J., Kirkpatrick, J.D., Brown, M.E., Reid, I.N., Burrows, A., Liebert, J., Matthews, K., Gizis, J.E., Dahn, C.C., Monet, D.G., Cutri, R.M., Skrutskie, M.F., 2002b, ApJ, 564, 421.

Burrows, A., Marley, M., Hubbard, W.B., Lunine, J.I., Guillot, T., Saumon, D., Freedman, R., Sudarsky, D., Sharp, C., 1997, ApJ, 491, 856.

Burrows, A., Hubbard, W.B., Lunine, J.I., Liebert, J. 2001, Rev. Mod. Phys., 73, 719.

Chabrier, G., Baraffe, I., 2000, ARA&A, 38, 337.

Chabrier, G., Baraffe, I., Allard, F., Hauschildt, P., 2000, ApJ, 542, 464.

Comerón, F., Neuhäuser, R., Kaas, A.A., 2000, A&A, 359, 269.

Comerón, F., Reipurth, B., Henry, A., Fernández, M., 2003, A&A, submitted.

Cooper, C.S., Sudarsky, D., Milsom, J.A., Lunine, J.I., Burrows, A., 2003, ApJ, 586, 1320.

Dahn, C.C., Harris, H.C., Vrba, F.J., Guetter, H.H., Canzian, B., Henden, A.A., Levine, S.E., Luginbuhl, C.B., Monet, A.K.B., Monet, D.G., Pier, J.R., Stone, R.C., Walker, R.L., 2002, AJ, 124, 1170.

Dickinson, M., Hanley, C., Elston, E., Eisenhardt, P.R., Stanford, S.A., Adelberger, K.L., Shapley, A., Steidel, C.C., Papovich, C., Szalay, A.S., Bershady, M.A., Conselice, C.J., Ferguson, H.C., Fruchter, A.S., 2000, ApJ, 531, 624.

Franx, M., Moorwood, A., Rix, H.-W., Kuijken, K., Röttgering, H., van der Werf, P., van Dokkum, P., Labbé, I., Rudnick, G., 2000, *The Messenger*, 99, 20.

de la Fuente Marcos, C., de la Fuente Marcos, R., New Astron., 4, 21.

Geballe, T.R., Saumon, D., Leggett, S.K., Knapp, G.R., Marley, M.S., Lodders, K., 2001, ApJ, 556, 373.

Kirkpatrick, J.D., Reid, I.N., Liebert, J., Cutri, R.M., Nelson, B., Beichman, C.A., Dahn, C.C., Monet, D.G., Gizis, J.E., Skrutskie, M.F., 1999, ApJ, 519, 802.

Labbé, I., Franx, M., Rudnick, G., Förster Schreiber, N.M., Rix, H.-W., Moorwood, A.F.M., van Dokkum, P.G., van der Werf, P., Röttgering, H., van Starkenburg, L., can de Wel, A., Kuijken, K., Daddi, E., 2003, AJ, 125, 1107.

Leggett, S.K., Geballe, T.R., Fan, X., et al., 2000, ApJ, 536, L35.

Leggett, S.K., Golimowski, D.A., Fan, X., et al., 2002, ApJ, 564, 452.

Lodders, K., 1999, ApJ, 519, 793.

Lucas, P.W., Roche, P.F., 2000, MNRAS, 314, 858

Lucas, P.W., Roche, P.F., Allard, F., Hauschildt, P.H., 2001, MNRAS, 326, 695.

Maihara, T., Iwamuro, F., Tanabe, H., 2001, PASJ, 53, 25.

Martín, E.L., Zapatero-Osorio, M.R., 2003, ApJ, 593, L113.

Persson, S.E., Murphy, D.C., Krzeminsky, W., Roth, M., Rieke, M.J., 1998, AJ, 116, 2475.

Reipurth, B., Clarke, C.J., 2001, AJ, 122, 432.

Renzini, A., Cesarsky, C., Cristiani, S., da Costa, L., Fosbury, R., Hook, R., Leibundgut, B., Rosati, P., Vandame, B., 2003, in The mass of galaxies at low and high redshifts, eds. R. Bender and A. Renzini, Springer-Verlag.

Saumon, D., Hubbard, W.B., Burrows, A., Guillot, T., Lunine, J.I., Chabrier, G., 1996, ApJ, 460, 993.

Smail, I., Owen, F.N., Morrison, G.E., Keel, W.C., Ivison, R.J., Ledlow, M.J., 2002, ApJ, 581, 844.

Stetson, P.B., 1987, PASP, 99, 191

Tinney, C.G. (ed.), 1995, The Bottom of the Main Sequence - and Beyond, Springer-Verlag.

Wichmann, R., Bastian, U., Krautter, J., Jankovics, I., Ruciński, S.M., 1998, MNRAS, 301, L39.

Zapatero Osorio, M.R., Béjar, V.J.S., Rebolo, R., Martín, E.L., Basri, G., 1999, ApJ, 524, L115.

Zapatero Osorio, M.R., Béjar, V.J.S., Martín, E.L., Rebolo, R., Barrado y Navascués, D., Bailer-Jones, C.A.L., Mundt, R., 2000, Science, 290, 103.

Zapatero Osorio, M.R., Béjar, V.J.S., Martín , E.L., Rebolo, R., Barrado y Navascués, D., Mundt, R., Eislöffel, J., Caballero, J.A., 2002, ApJ, 578, 536.

This manuscript was prepared with the AAS LaTeX macros v5.0.

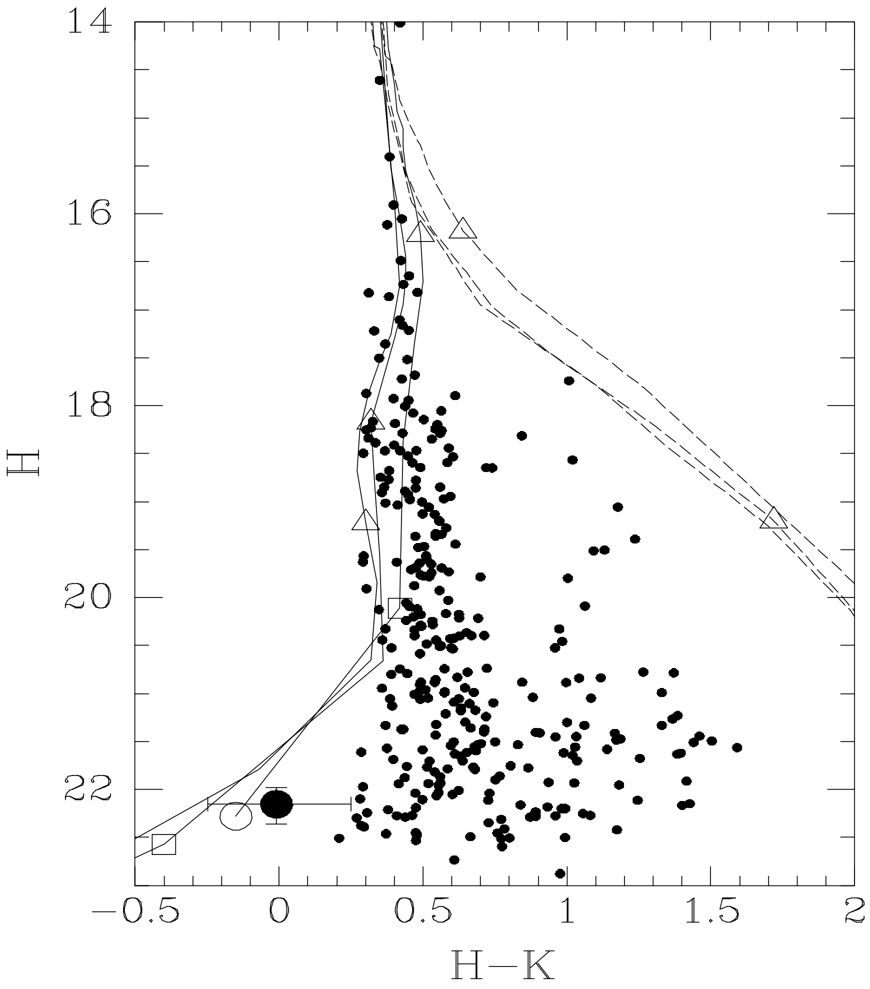

Fig. 1.— $(H - K_S, H)$ color-magnitude diagram of the objects detected in our images. Only objects exceeding a detection threshold of 5σ in our H band images are plotted. ChaI J110814.2-773649 is the point at the bottom left with error bars plotted on it. The curves are theoretical isochrones for ages 1 Myr, 5 Myr, and 10 Myr according to two different sets of models (see Section 3.2.2) at the distance of Chamaeleon I. The dashed lines correspond to the DUSTY models of Chabrier et al. (2000), in which dust grains form and stay in the atmosphere. The solid lines correspond to the COND models (Baraffe et al. 2003), in which dust grains precipitate under the photosphere as soon as they are formed. The latter set of models is expected to better represent the cool ($T \sim 1000$ K) objects of interest in this work. The symbols plotted on the curves denote the position of objects of different masses at the age of each isochrone: triangles correspond to 5 M_{Jup}, squares to 1 M_{Jup}, and circles to 0.5 M_{Jup}. The large overlap among the isochrones corresponding to each model implies a large degeneracy between age and mass. The red, bright object near the dashed curves at H = 17.74, $H - K_S$ = 1.01 is not a candidate L dwarf, but a well resolved elliptical galaxy

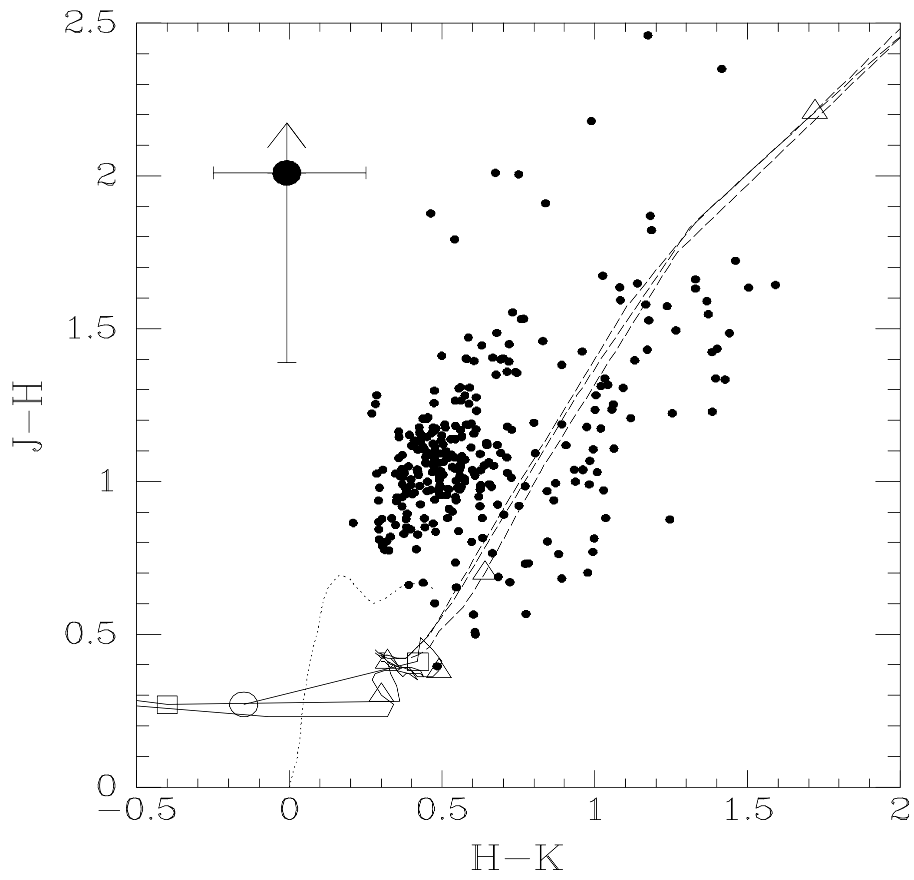

Fig. 2.— $(H-K_S, J_S-H)$ diagram of all objects having H-band detections at a level higher than 5σ in our images. ChaI J110814.2-773649 is the point at the upper left with error bars plotted on it. Solid and dashed lines, and the empty symbols along them, represent theoretical isochrones as in Figure 1. The dotted line is the *locus* of dwarf stars between spectral types B and M6 from Bessell and Brett (1988). The displacement between the highest density of points in the diagram, corresponding to stars background to the Chamaeleon I cloud, and this *locus* is due to the moderate extinction caused by the dust in the star forming region that pervades the imaged area.

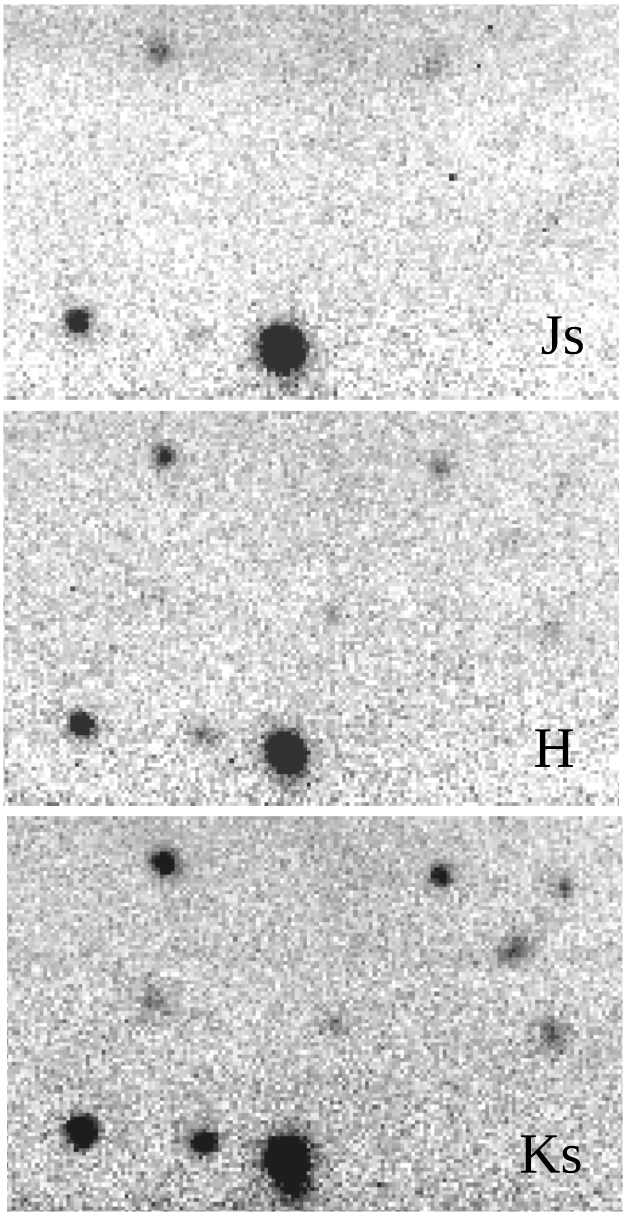

Fig. 3.— Images of ChaI J110814.2-773649 in the J_S, H, and K_S bands. This is a small portion ($23'' \times 15''$) of the field imaged in our observations. ChaI J110814.2-773649 is the faint object in the center of the images.

Fig. 4.— Combined frame containing the VLT/ISAAC spectrum of ChaI J110814.2-773649. The white trace in the upper part corresponds to the bright reference star, and the arrow marks the expected position of the trace of the spectrum of ChaI J110814.2-773649. The black stripes are artifacts of the data reduction. The spectrum ranges from 1.4 μm (left) to 1.8 μm (right) and is strongly binned along the dispersion direction to enable detection of the $H = 22.16$ object. See Section 2.2 for a detailed explanation of the reduction process.

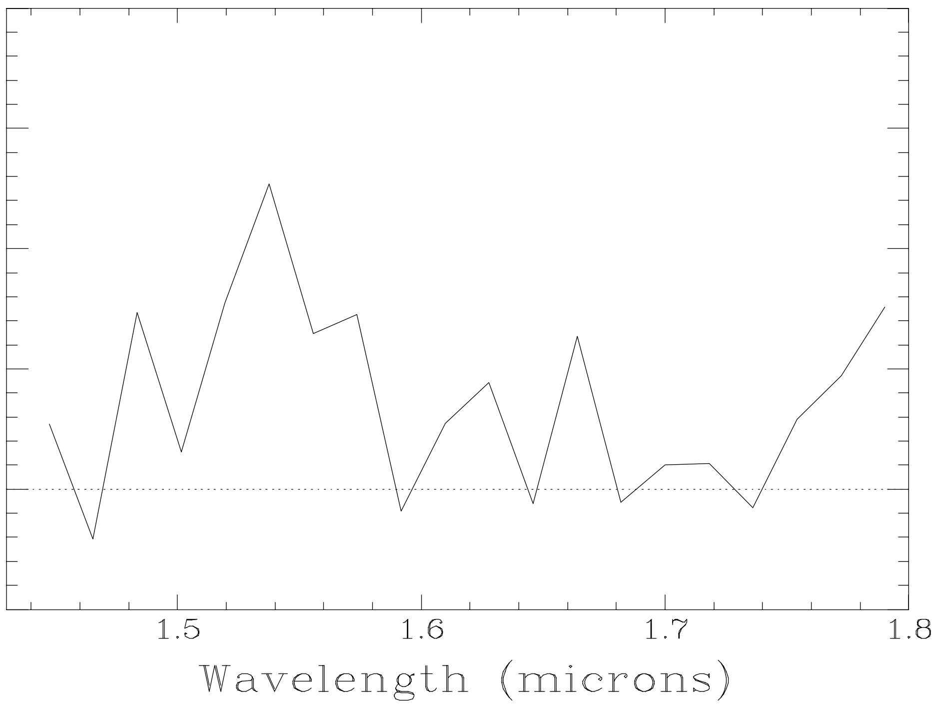

Fig. 5.— Extracted spectrum of ChaI J110814.2-773649. Relative flux calibration was achieved by ratioing its binned spectrum by that of the bright reference star included in the slit, multiplying by the ratio between a spectrum of this star and that of the B4V star HD 94414 observed one after another at similar mass degraded to the same resolution, and then multiplying by a $T = 17,200\ K$ blackbody that approximates the spectral energy distribution of HD 94414. The lower dotted line marks the zero flux level.